Chapter 4: Investigating the role of *Plasmodium falciparum* genetic background in tolerance to artemisinin-resistance *Pfkelch13* mutations and assessing human kelch inhibitors for antimalarial activity on *Pfkelch13*

4.1 Summary

The first aim of this chapter is to test the effect of different genetic backgrounds on the acquisition of artemisinin resistance. The hypothesis is that strains with existing artemisinin resistance will have a higher likelihood of acquiring a resistance allele of *Pfkelch13* compared with sensitive parasites, due to previous adaptations. This question will be tested by triggering a double-strand break at the key C580 codon using Cas9, and providing multiple possible template for repair. To create the mix of donor templates, I aimed to generate new pools of *Pfkelch13* donor plasmids for CRISPR editing of the C580 codon. From a comprehensive pool of all 64 possible codons, I aimed to isolate plasmids of donors that encode for only viable alleles incorporated in 580 of *Pfkelch13* and exclusion of plasmids with "non-compatible" donors in the pool based on previous transfection data. Using sub-pools of only donors that are compatible with viability, this should lead to increased transfection efficiency at a larger scale thus allowing the investigation of tolerance of resistance-associated mutations in different genetic backgrounds.

The second aim of this chapter was to determine the potential antimalarial activity of inhibitors of human kelch-like ECH-associated protein 1 (KEAP1) on *P. falciparum* parasites including whether there was differential activity on parasites harbouring *Pfkelch13* mutations.

4.2 Background

4.2.1 Parasite fitness and drug resistance:

The reduction in malaria morbidity and mortality has been achieved by use of ACTs as frontline treatment which consist of artemisinin and partner drugs. This progress in malaria control is however threatened by the increasing prevalence of *P. falciparum* parasites with decreased sensitivity to artemisinin that has emerged at various locations in South East Asia over the last decade, and recent emergence in Africa (Siddiqui *et al,* 2020). The efficacy of previous frontline antimalarials such as chloroquine has historically been hindered by emergence of drug resistance with a similar pattern of resistance emergence and spread in different endemic regions (Uwiman *et al,* 2020). The occurrence of point mutations in the Kelch propeller domain of *Pfkelch13*, has been associated with artemisinin resistance. However, there is no definitively established mechanism of artemisinin resistance, which has been linked to an activated unfolded protein response, altered DNA replication, increased levels of phosphatidylinositol 3-phosphate, reduced protein translation and increased cellular stress (Birnbaum *et al,* 2020). Assessing the prevalence of molecular markers associated with therapeutic efficacy of artemisinin and its partner drugs for continuous systematic, conscientious monitoring of anti-malarial drug resistance is necessary to ensure the continuous use of efficacious ACTs (Raman *et al,* 2019).

Several *Pfkelch13* mutations have been identified in various malaria endemic regions with only a few validated to incur artemisinin resistance from *in vitro* experiments. The C580Y allele has become the most prevalent allele, replacing other circulating mutations of *Pfkelch13* in multiple Southeast Asian regions, and has also been detected in Africa and South America. The mutation has been validated both *in vitro* and *in vivo* as having a role in artemisinin resistance (Stokes *et al,* 2021; Miotto

et al, 2020). Mutations in other genes, which have been suggested to either contribute to a multigenic basis of resistance or fitness, or serve as genetic markers of founder populations, have also been associated with artemisinin resistance in *Pfkelch13* mutant parasites. This includes mutations in ferredoxin *(fd),* multidrug resistance protein 2 *(mdr2)* and *plasmepsin 2-3* that is associated with piperaquine resistance in dihydroartemisinin-piperaquine treatment failure (Apinjoh *et al,* 2019; van der Pluijm *et al,* 2019).

Plasmodium kelch13 mutations have been observed at a low frequency in regions including Africa and South America but have been occurring at an increasing prevalence in Southeast Asia over the past decade (Cerqueira *et al,* 2017). Several non-synonymous mutations with multiple independent origins have been associated with artemisinin resistance since its emergence in early 2000s. The C580Y allele is one of the four Asian mutations (C580Y, R539T, I543T, and Y493H) validated *in vitro* and *in vivo* that are rarely reported in other endemic regions. The C580Y mutation has become the most implicated allele that has occurred and spread in higher frequency in Asia (Anderson *et al,* 2016; Mernard *et al,* 2016). A multidrug-resistant lineage harbouring the *Pfkelch13* C580Y has been reported to spread and nearly reached fixation in Southeast Asian regions such as Cambodia, East Thailand and Vietnam, indicating the rapid invasion of the C580Y allele of the population (Coppée *et al,* 2019; Ariey *et al,* 2013). The C580Y SNP in the *Pfkelch13* gene has been shown to play a dominant role in artemisinin resistance in multiple regions with independent origins of the mutation reported (Miotto *et al,* 2020; Zaw *et al,* 2020). The enhanced fitness of *Pfkelch13* C580Y compared to other *Pfkelch13* mutations is suggested to be the main factor of its dominance instead of the level of resistance conferred. This is suggested by *in vitro* studies in isogenic backgrounds in which parasites harbouring *Pfkelch13*

R539T or I543T mutations that conferred the highest levels of artemisinin resistance were outcompeted by C580Y mutated parasites (Gnädig *et al,* 2020; Straimer *et al,* 2015).

Understanding the aspects of parasite genetic background and co-segregating compensatory mutations with varying impacts on observed fitness costs of artemisinin resistant parasites is essential in understanding mechanisms of resistance in ACTs (Tirrel *et al,* 2019; Amato *et al,* 2020). Factors driving the increased substitution rate of tyrosine with cysteine at position 580 in the *Pfkelch13* gene resulting in the C580Y allele, are yet to be well established. However, the success of C580Y and impact on parasite fitness may be explained by epistatic interactions with other variants and genetic background that has been suggested to play an important role in frequencies of some *P. falciparum* SNPs (Nair *et al,* 2018; Straimer *et al,* 2017).

4.2.2 Kelch-like ECH-associated protein 1 (KEAP1)

Kelch-like ECH-associated protein 1 (KEAP1) is a highly conserved dimeric protein, consisting of 624 amino acids, that is rich in cysteine and shares 92% sequence homology among the mammalian species (Naidu *et al,* 2020). The human KEAP1 is a component of the Cullin 3 (CUL3)-based E3 ubiquitin ligase complex that is involved in the activation of nuclear factor erythroid 2-related factor 2 (NRF2) protein (Taguchi and Yamamoto, 2017). NRF2 and KEAP1 are the key signalling proteins in the KEAP1-NRF2 pathway that regulates cytoprotective responses resulting from oxidative stress (Kansanen *et al,* 2013). The KEAP1-NRF2 protein-protein interaction is involved in several diseases of oxidative stress and inflammation including lung, liver, kidney, gastrointestinal (GI) tract and cardiovascular system diseases, neurological conditions, metabolic, inflammatory and autoimmune

disorders. Expression of critical enzymes involved in the synthesis and use of redox buffer reduced glutathione, and many ancillary proteins within the redoxin family, are regulated by NRF2 thus controlling production of reactive oxygen species (Baird and Yamamoto, 2020; Cuadrado *et al,* 2019). However, enhanced survival and proliferation of cancer cells has also been reported to occur due to elevated NRF2 activity.

Due to the major involvement of the KEAP1-NRF2 signalling pathway in these diseases, this system has become a potential therapeutic target. In addition to the development of modulators of NRF2 for this purpose, compounds that target KEAP1 as a main regulator of NRF2 degradation have also been developed (Cuadrado *et al,* 2019; Qin *et al,* 2019; Deshmukh *et al,* 2016). Some of these molecules developed to target KEAP1 have been reported to have very high affinity for, and are inhibitors of, the C-terminal Kelch/β-propeller domain of KEAP1. This KEAP1 Kelch/β-propeller domain through which KEAP1 binds to NRF2 is one of the major functional domains of KEAP1 (Lu *et al,* 2019; Robledinos-Antón *et al,* 2019). There is significant similarity in the structures (Figure 4.1) of the KEAP1 Kelch/β-propeller domain and kelch13 of *P. falciparum* that is associated with resistance to artemisinin derivatives. The potential activity of reported KEAP1 inhibiting compounds against *P. falciparum* was assessed in this chapter.

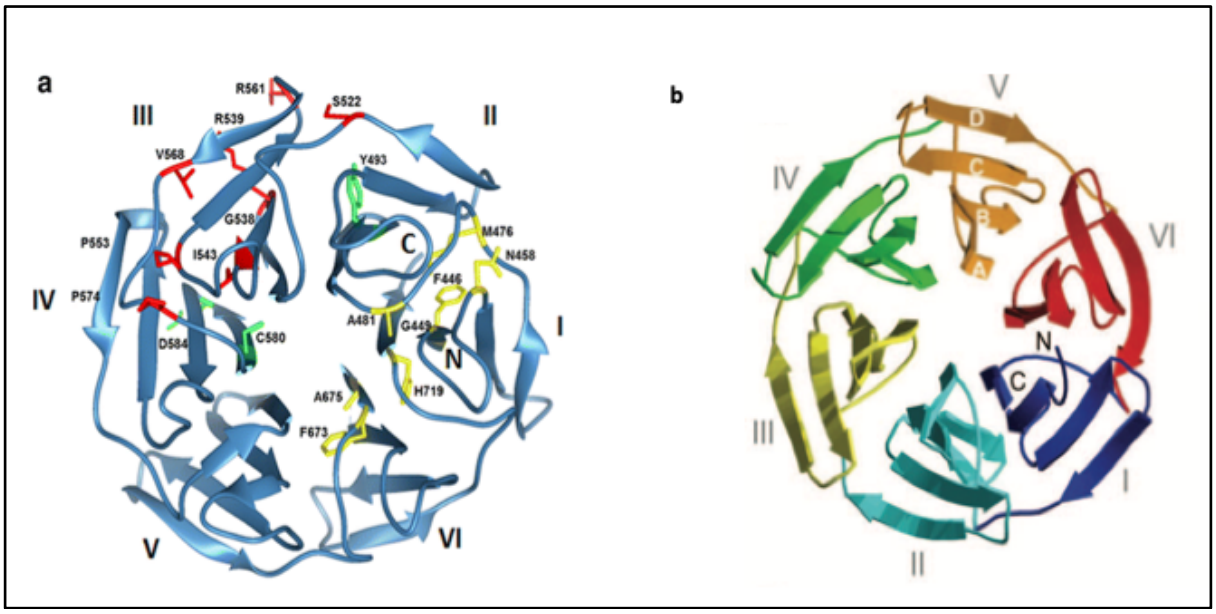

Figure 4.1 Schematic representation of KEAP1 kelch and *Pfkelch13* domains consisting of 6 blades (I – VI). a) The propeller domain of *Pfkelch13* and artemisinin resistance mutations in the propeller domain. Residues in clusters I and II are coloured red and yellow respectively; green coloured residues are not in any cluster. **b)** the kelch domain of KEAP 1; the four β-strands labelled A-D on each blade and the N and C termini located in blade I. Figures from Singh *et al* (2016) and Li *et al* (2004)

4.2.3 CRISPR/Cas9 plasmids design

As part of Manuela Carrasquilla's PhD project (2019), CRISPR/Ca9 plasmids harbouring different donor templates were designed to perform saturation mutagenesis at position 580 of *Pfkelch13* in parasites of different strains. The donor sequences of the plasmids were designed to also include synonymous 'shield' mutations at the cleavage site close to the PAM. This protects the modified sequence to prevent further cleavage by the Cas9 nuclease with a gRNA designed and cloned to target *Pfkelch13*. These plasmids contained a common pDC2 backbone with a codon-optimised Cas9 driven by a calmodulin promoter from *P. falciparum*, a hDHFR selectable marker, a U6 cassette for the expression of a single gRNA and a K13 donor sequence for homologous recombination (pDC2-coCas9-U6-K13-C580NNN-hDHFR). This template was synthesised to contain a homology sequence with the potential to encode any codon at position 580 to generate all possible mutant

Pfkelch13 lines, in effect mimicking spontaneous mutations due to random codon repair at this position. This was facilitated by synthesis of a gBlock template with NNN specified at position 580. All possible 64 donors were represented within the pool of plasmids where NNN represents any possible codon to replace 580. This complex mixture of plasmids representing all possible amino acids was assessed using amplicon sequencing to determine the proportions of each of the 64 codons in the pool.

Manuela Carrasquilla used this complex pool of plasmids with mutations at position 580 of *Pfkelch13* to transfect parasites of different strains. Transfections initially measured by PCR and Sanger sequencing, were assessed by Next Generation Sequencing to determine the proportion of each amino acid for each transfection. Tyrosine (Tyr) was only obtained in a Cambodian isolate (CAM) of the KEL1 lineage described by Amato *et al,* 2018, and not in any of the other genetic backgrounds. Multiple codons including the reference allele, cysteine (Cys), were successfully incorporated at position 580 in the other genetic backgrounds using this approach (Figure 4.2) performed by Manuela Carrasquilla. However, the vast majority of transfections were unsuccessful, likely due to the presence of non-viable codons in the mix. I intended to deconvolute this complex pool of plasmids to isolate individual donors to be used in generating new sub-pools of *Pfkelch13* C580 plasmids.

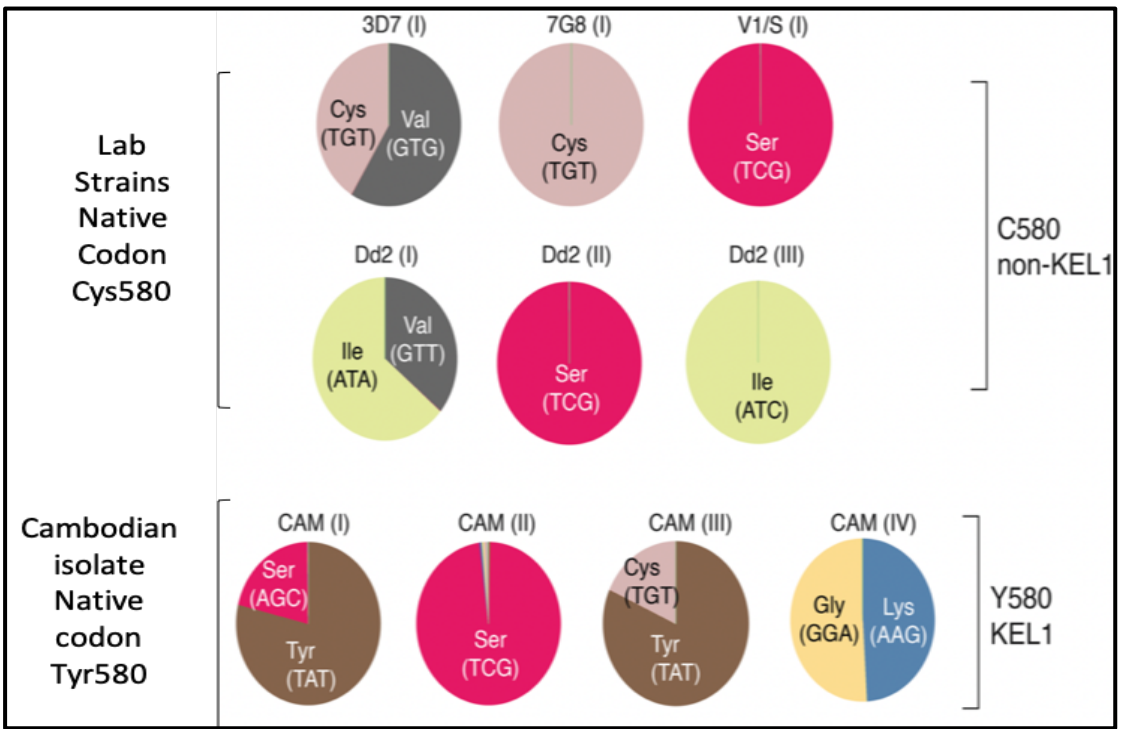

Figure 4.2 Codon substitutions at position 580 from transfections with the complex pool of plasmids. The proportion of each codon observed in independent transfections across the different *P. falciparum* lab strains (3D7, 7G8, V1/S, and Dd2) harbouring cysteine (C580) and CAM strain harbouring tyrosine (Y580) as the original haplotype at position 580. Each pie chart represents the outcome from a single transfection, and shows the proportion of each residue observed in the bulk culture. Thus 3D7(i) indicates that this transfection of 3D7 returned predominantly valine and to a lesser extent cysteine. Tyrosine substitution and phenylalanine (not shown in the picture) were only observed in the CAM strain that is artemisinin resistant. Figure adapted from Manuela Carrasquilla (2019).

4.3 Methods and Results

Multiple techniques, illustrated in figure 4.3, were performed to generate new sub-pools of plasmids with only compatible donors of “viable”, previously observed alleles from the complex pool for enhanced transfection efficiency of parasites of different genetic backgrounds This was aimed at facilitating assessment of tolerance and impact on fitness of *Pfkelch13* mutations in these strains.

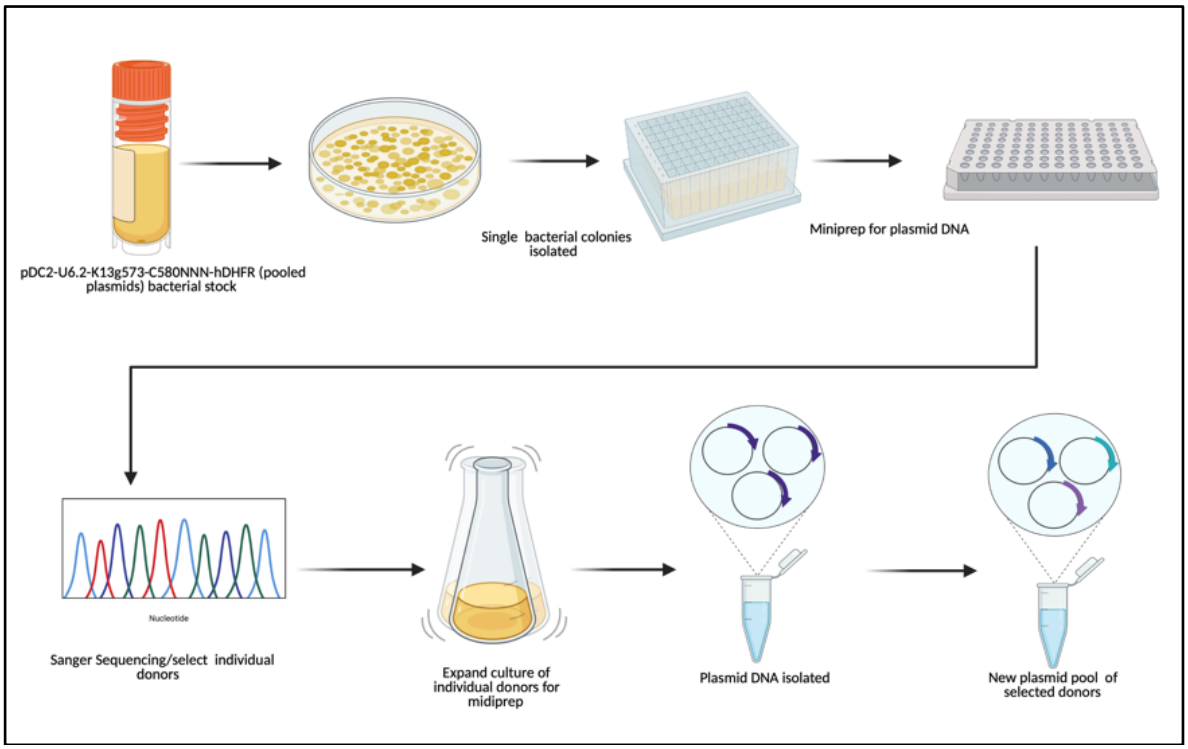

Figure 4.3 Schematic representation of the generation of new plasmid sub-pools. The workflow of deconvoluting the complex pool of plasmids from bacterial stock to isolate and select individual donors is shown

4.3.1 Deconvolution of a complex pool of plasmids

To deconvolute the complex pool of plasmids, plasmid DNA was isolated from 116 single individual bacterial colonies from the bacterial glycerol stock of the complex pool using the methods described in section 2.5.3. In order to identify individual plasmids with amino acids encoding for the donors of interest (Table 4.1), Sanger sequencing was performed on isolated plasmid DNA and the reads were aligned to K13-C580NNN donor sequences and analysed using SeqMan Pro software on DNASTAR Navigator. The chromatograms of the region around 580 of *Pfkelch13* were used to determine the codon replacing 580 in each isolated plasmid (examples shown in Figure 4.4). Plasmids with any of the target codons with no other mutation in the sequences in the *Pfkelch13* region were selected for use in generating the new pool.

Besides the donors with the codons of interest, several other codons encoding for various amino acids were obtained (Figure 4.5), including multiple codons encoding for the same amino acid. The occurrence of multiple codons from the deconvolution of the pooled plasmids supports the efficiency of design of the previously mentioned gBlock for introduction of spontaneous mutations.

The isolated plasmids with the donor of interest were inoculated in larger volumes and Midipreps performed for plasmid DNA isolation, described in section 2.5.4, with final elution in sterile cytomix ready for transfection.

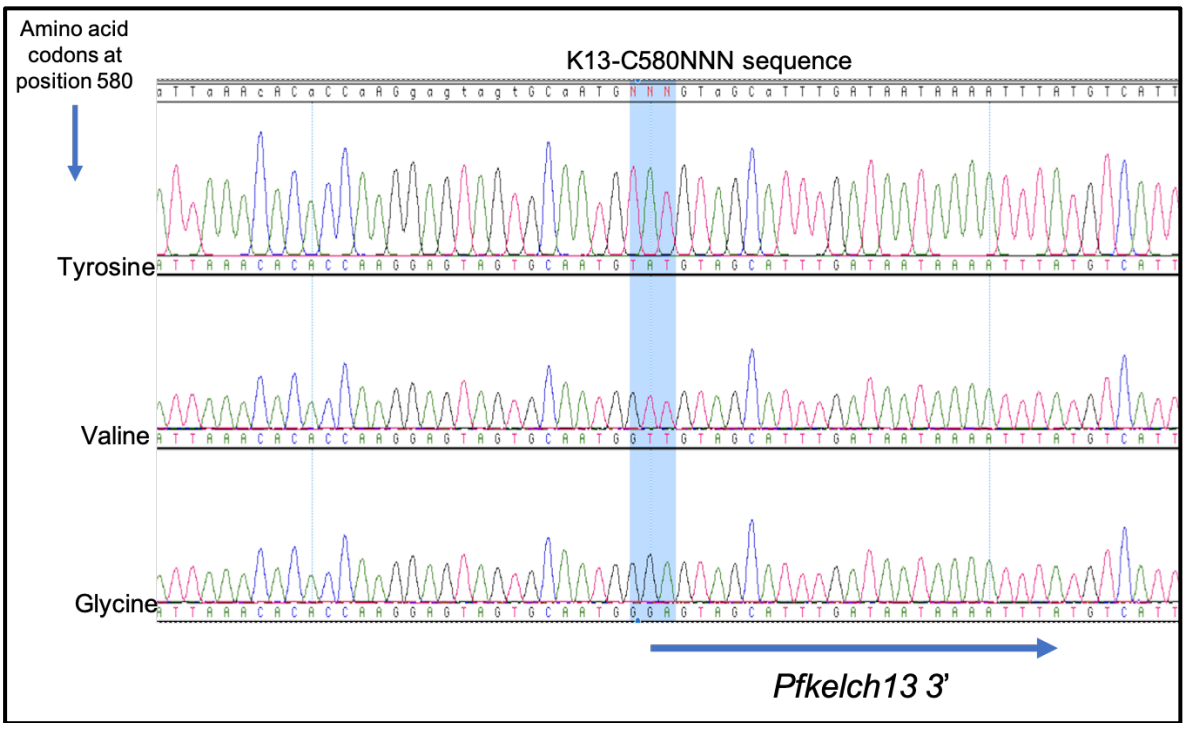

Figure 4.4 Chromatogram from Sanger sequencing of isolated plasmids. Donor sequence, with position 580 highlighted in blue, encoding for some of the donors of interest. The sequences were aligned with the K13-580NNN donor sequence (above).

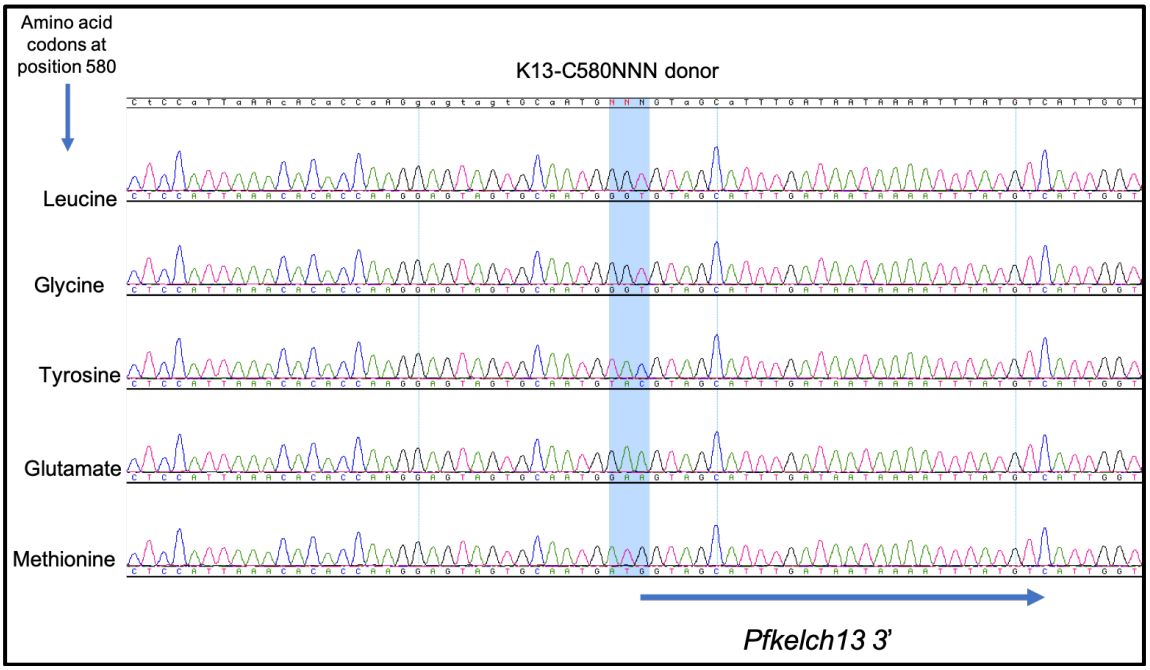

Figure 4.5 Chromatogram from Sanger sequencing of individual plasmids. Donor sequence at position 580 encoding for some of the donors of interest and other codons not included in the sub-pool of plasmids.

4.3.2 Identification of individual donors to generate a plasmid sub-pool

Donor plasmids with multiple codons encoding for various amino acids were isolated upon deconvolution of the complex plasmid pool. The results obtained for frequencies of the different amino acids from the deconvoluted complex pool indicates the representation of different codons in the original donor pool. This supports the findings by Manuela Carasquilla in which most codons were found to be represented fairly equally by amplicon sequencing of the original donor pool. Only a subset of codons encoding for leucine was found at a lower abundance (Manuela Carrasquilla, PhD 2019). In addition to the target donors of interest, a number of other donors with diverse codons (Table 4.1) at position 580 were also isolated, with some occurring at relatively high frequency. Donors encoded for by a multiple different codons and donors encoded for by a single codon were all represented in the total number of individual plasmids isolated. Altogether, 51 codons out of the possible 64 were

identified. The individual codons encoding for the amino acid serine (C580S allele) and glycine (C580G), which were two of the target donors for the sub-pool, occurred at the highest frequency, consistent with their being encoded by six and four codons respectively and their relative abundance in the original pool.

Table 4.1 Amino acid codons obtained from isolated individual donors. The different amino acids and their codons from each of the individual donors after isolation from the mixed pool. Targeted amino acids that represent known viable codons used to make a new plasmid sub-pool are highlighted in bold

Amino Acid	Codon
Glutamate (Glu)	GAG, GAA
Arginine (Arg)	AGA, CGT, CGA, CGG, AGG
Termination (Ter)	TAA, TGA, TAG
Proline (Pro)	CCA, CCC
Threonine (Thr)	ACA, ACT, ACG
Leucine (Leu)	TTG, CTA
Histidine (His)	CAC, CAT
Asparagine (Asp)	AAT, AAC
Phenylalanine (Phe)	TTC, TTT
Aspartate (Asp)	GAC, GAT
Glutamine (Gln)	CAA
Isoleucine (Ile)	ATC
Tryptophan (Trp)	TGG
Alanine (Ala)	GCA, GCC
Valine (Val)	GTG, GTT, GTA, GTC
Methionine (Met)	ATG
Cysteine (Cys)	TGT, AGT
Lysine (Lys)	CGA, AAA, AAG
Glycine (Gly)	GGG, GGT, GGA, GGC
Serine (Ser)	TCA, TCG, TCC, AGT
Tyrosine (Tyr)	TAT, TAC

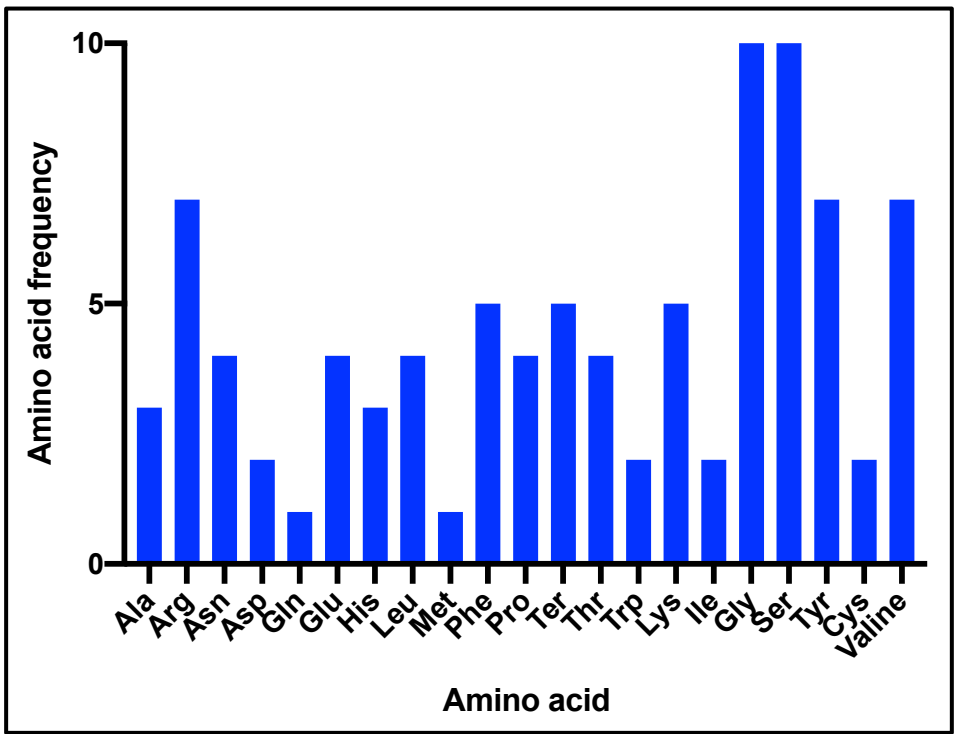

Figure 4.6 Frequency of the different amino acids in the isolated plasmids. The occurrence of the different amino acids from isolated donors with codons for glycine and serine occurring the highest frequency. Termination/stop codons were also isolated.

4.3.3 Transfection of *P. falciparum* parasites with plasmid sub-pool

Plasmid DNA was quantified using the NanoDrop ND-1000 UV-Vis Spectrophotometer (ThermoFisher Scientific) and a new pool of the plasmid consisting of donors encoding the known viable codons (cysteine, lysine, glycine, valine, isoleucine, phenylalanine, tyrosine and serine) was prepared with each plasmid at equal stoichiometric amounts, with a final concentration of 50µg/mL in the final mixture. *P. falciparum* parasites have been shown to have the ability of efficiently taking up multiple plasmids in co-transfections (Carrasquilla *et al,* 2019; Ghorbal *et al,* 2014).

In addition to testing Southeast Asian backgrounds, I planned to examine the impact of *Pfkelch13* mutations in African parasite backgrounds (see Table 2.1 in methods). Transfections were performed with the Southeast Asian lab line, Dd2,

African strains FCR3 (from The Gambia) and a recent isolate from Tanzania (Tanzania-200708). These parasites were transfected using the plasmid sub-pool of multiple *Pfkelch13* 580 donors generated. The transfections were performed in two duplicates of two independent batches. To assess transfection efficiency, these same strains were transfected in parallel with a control plasmid pDC2-ef1a-Vps4wt-mRFP/hDHFR, expressing the mRFP fluorescent reporter. Transfections of parasites were performed using the method described in section 2.4. Transfected parasites were maintained in culture with WR99210 to select for plasmid-containing parasites. WR99210 is a compound that blocks production of tetrahydrofolate in the folate pathway by acting against parasite bifunctional dihydrofolate reductase thymidylate synthase enzyme (DHFR-TS) but not human DHFR. WR99210 is widely used for selection of transfectants due to elevated IC_{50} in *P. falciparum* parasites transformed with expressing episomal expression of the hDHFR coding sequence. This has made hDHFR a powerful selectable resistance marker for transfection of *P. falciparum* parasites (Remcho, *et al,* 2020; Fidock and Wellems, 1997).

Culture of the transfected lines with the plasmid sub-pool were maintained as described in section 2.14 up to day 32 and day 12 post-transfection for the two independent transfections done with the C580 plasmid sub-pool, respectively. However due to the closures of the laboratories as result of the Covid-19 outbreak these transfections were discontinued. Dd2 parasites transfected with the control plasmid pDC2-ef1a-Vps4wt-mRFP/hDHFR were however recovered at day 16 post-transfection when parasites became visible by microscopy.

There was no recovery of parasites in the transfected field strains FCR3 and Tanz 200708 in both transfections done with the control plasmid and the plasmid pool of K13 mixed donors, although this was challenged by the disruption of the

experiments from the closure of laboratories. However, while Dd2 returned parasites on day 16 with the control plasmid (pDC2-ef1a-Vps4wt-mRFP/hDHFR, an episomal plasmid expressing an mRFP-tagged protein), the other two lines transfected with control plasmid in parallel with Dd2 did not return parasites by day 57 post-transfection suggesting that they are more challenging to transfect.

4.3.4 Assessing antimalarial activity of Kelch-like ECH-associated protein 1 (KEAP1) inhibitors

Due to time constraints upon reopening of the laboratory, this part of the project was refocused to explore whether small molecules would be able to differentially target wild type and mutant *Pfkelch13*. Although no compounds targeting *Pfkelch13* have yet been described, human Kelch-like proteins have been the subject of drug development efforts as described in the Introduction. In order to assess if compounds known to inhibit the Kelch-like ECH-associated protein 1 (KEAP1) have potential antimalarial activity on *P. falciparum* parasites, standard 72-hour drug sensitivity assays were performed.

4.3.4.1 Drug Sensitivity Assays using Keap1 inhibitors

Standard 72-hour antimalarial drug sensitivity assays were performed using compounds that are known to inhibit the kelch domain of Keap1 following methods described in section 2.3.1 and 2.3.2. This was performed to investigate the potency of these compounds against *P. falciparum* parasites. The IC_{50} value, which is the concentration of the compound required to inhibit 50% of parasite growth to determine response to a drug, was measured for compounds KI696, RA839 and ML334 as described below. The assay was performed to determine IC_{50} values against

laboratory adapted *P. falciparum* strains 3D7 and Dd2 wild type (WT) and Dd2 *Pfkelch13* edited mutants harbouring R539T and C580Y mutations. This rapid and cost-effective method has been applied over the past years, to determine potency of drugs by measuring growth inhibition in vitro using several DNA intercalating dyes like SYBR Green 1. SYBR Green dye binds directly to double stranded DNA allowing the measurement of DNA amount as a result of the detection of fluorescence signals from the SYBR Green intercalation with parasite DNA. Parasite growth which is inhibited by therapeutic concentrations of antimalarial drugs is measured by this fluorescence intensity (Dery *et al,* 2015; Karl *et al,* 2009).

The first KEAP1 kelch inhibiting molecule tested was KI696 that has been shown to demonstrate tight and selective binding to the kelch domain of KEAP1 by Davies *et al,* (2016) using fragment-based drug discovery. This molecule exhibited high potency and activation of the in human cell-based assays NRF2 pathway in vivo (Davies *et al,* 2016). The second compound RA839, with the chemical name (3S)-1-[4-[(2,3,5,6-tetramethylphenyl) sulfonylamino]-1-naphthyl] pyrrolidine-3-carboxylic acid, was reported to demonstrate non-covalent binding characteristics to the kelch domain of KEAP1 by Winkel *et al* (2015). RA839 was observed to be a selective inhibitor of the Keap1/Nrf2 interaction with a high affinity between the naphthalene ring system of RA839 bound to the central solvent channel of the kelch domain. Other KEAP1 kelch binding sites of RA839 formed by residues including Tyr334, Phe577, and Tyr572 at the hydrophobic and aromatic pocket and were also observed (Winkel *et al,* 2015).

The third KEAP1 inhibiting compound tested against *P. falciparum* was ML334 that is also referred to as LH601A with the chemical name (1*S*,2*R*)-2-[[(1*S*)-1-[(1,3-Dihydro-1,3-dioxo-2*H*-isoindol-2-yl) methyl]-3,4-dihydro-2(1*H*)-isoquinolinyl] carbonyl]

cyclohexanecarboxylic acid. The ML334 molecule, a stereoisomer (SRS)-5, was reported to demonstrate an inhibiting characteristic of Keap1-Nrf2 interaction by Hu *et al* (2014) dissociating NRF2 from KEAP1. The presence of the free carboxylic group of ML334 was observed to result in high affinity of ML334 isomer to the Nrf2 peptide binding site kelch domain of KEAP1 (Hu *et al,* 2013). The chemical structures of KI696, RA839 and ML334 are shown in Figure 4.7.

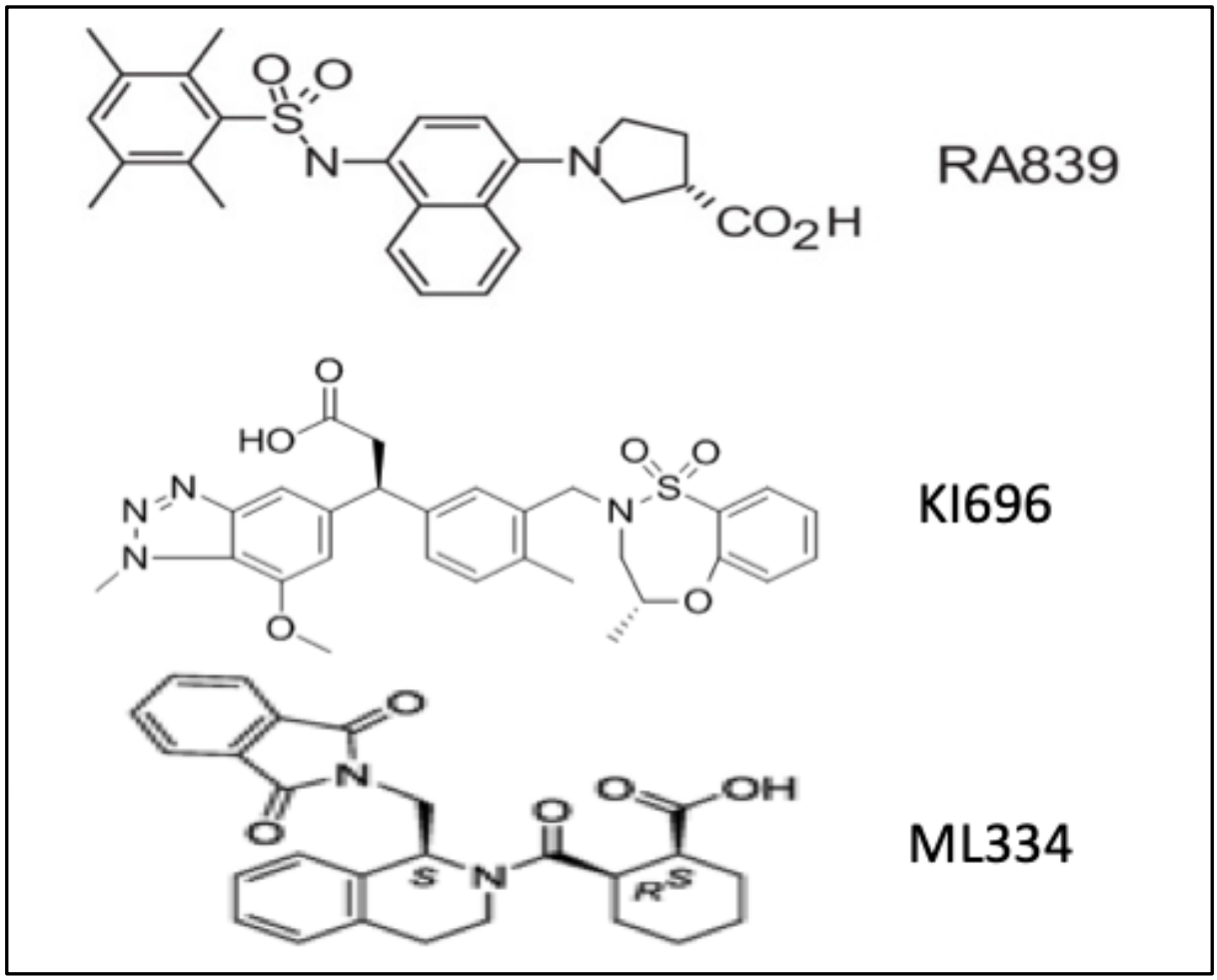

Figure 4.7 Chemical structure of KEAP1 kelch-inhibiting compounds. The structural difference of RA839, KI696 and ML334 (LH601A). (Davies *et al,* 2016; Winkel *et al,* 2015; Hu *et al,* 2104)

4.3.4.2 *Plasmodium falciparum* sensitivity to KEAP1 Kelch inhibitors

The drug-response curves for KI696, RA839 and ML334 were experimentally obtained in triplicates. Analysis was done on GraphPad Prism software and IC_{50}

values were established with a non-linear regression analysis generating the drug dose response curve. Activity against parasite growth in *P. falciparum* strains was demonstrated by all three compounds that were tested. Of the three compounds, ML334 was the most potent, with an IC_{50} of 1.7μM against 3D7, although the multi-drug resistant Dd2 strain had a higher IC_{50} of 5.2μM (Table 4.2 and Figure 4.10). In contrast, the other two compounds KI696 and RA839 showed only a slight shift with the IC_{50} for 3D7 marginally higher than Dd2 (Table 4.2, and Figures 4.8 and 4.9).

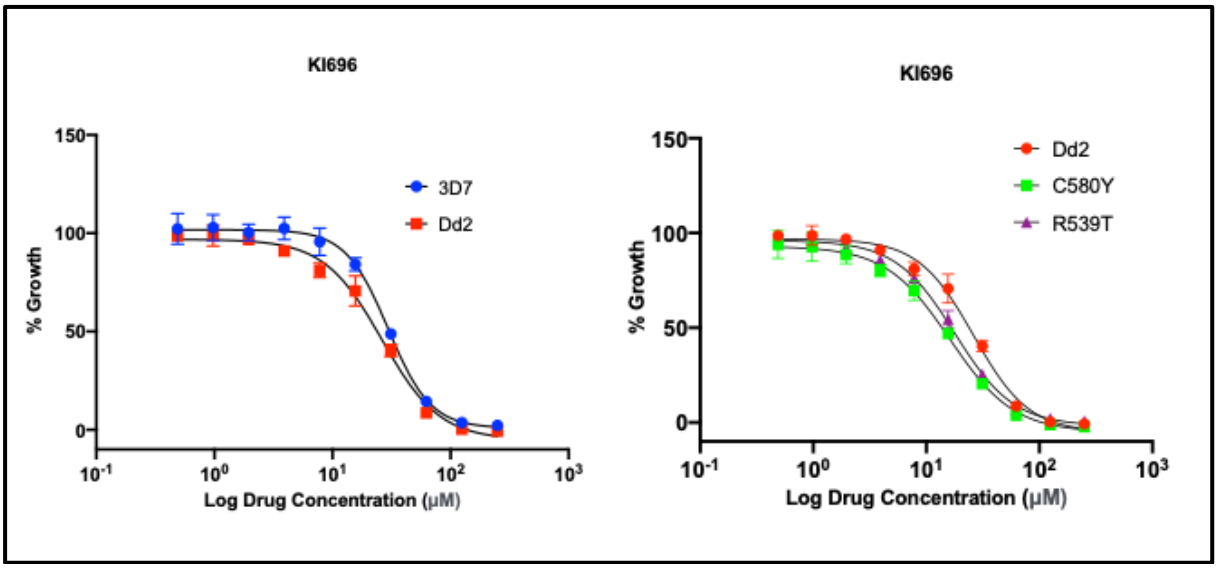

Figure 4.8 KI696 standard dose response curve. Dose response curves for the wild types (3D7 and Dd2) and Dd2 *Pfkelch13* mutants. A representative assay (technical triplicates) is shown. Similar IC_{50} curves were observed in the two biological replicates.

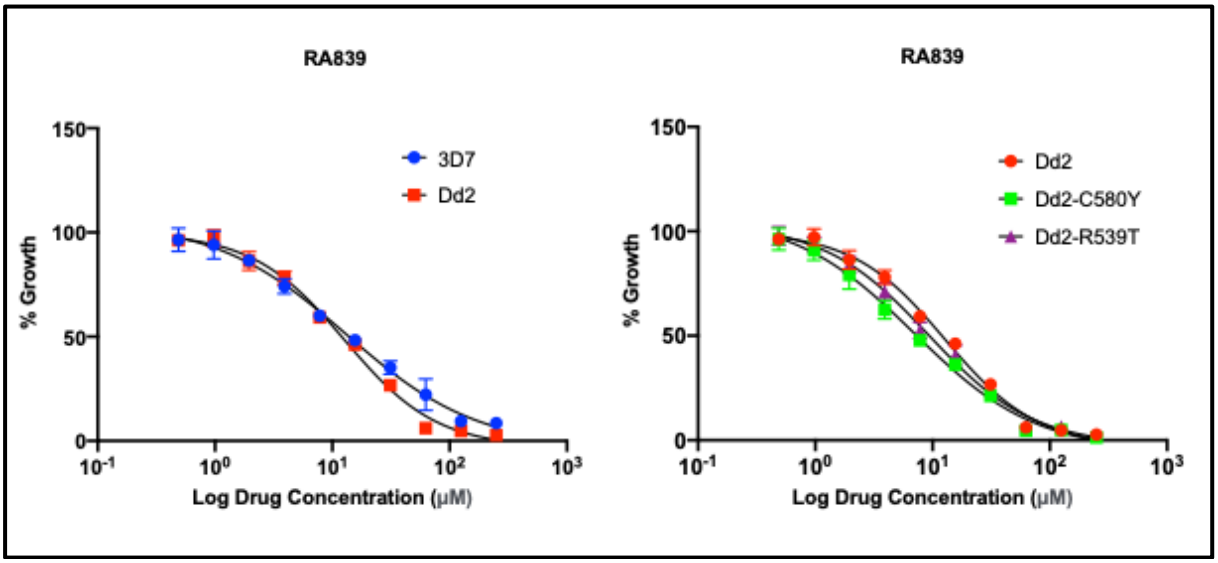

Figure 4.9 RA839 standard dose response curve. Dose response curves for the wild types (3D7 and Dd2) and Dd2 *Pfkelch13* mutants. A representative assay (technical triplicates) is shown. Similar IC_{50} curves were observed in the two biological replicates.

Table 4.2 The IC_{50} values obtained for compounds KI696, RA839 and ML334. Standard 72-hour drug assays were performed and the IC_{50} values obtained from biological duplicates of wild type strains and Dd2 mutant lines harbouring *Pfkelch13* mutations.

Compound	3D7 IC_{50} (μM)	Dd2 IC_{50} (μM)	Dd2-C580Y IC_{50} (μM)	Dd2-R539T IC_{50} (μM)
KI696	30.3	23.2	18.2	19.6
RA839	27.6	18.3	17.4	13.2
ML334	7	14	20.1	20.2

Interestingly, the Dd2 *Pfkelch13* mutant parasites, Dd2-C580Y and Dd2-R539T, showed increased sensitivity to KI696 and RA839, with the IC_{50} values lower than for the wild type Dd2. In contrast, the results obtained with the ML334 compound (Figure 4.10) demonstrated higher sensitivity by the wild type parasite than the Dd2 *Pfkelch13* mutant lines. Overall, however the highest fold shift of IC_{50} values in the Dd2 mutants compared to wild type Dd2 was < 2-fold for all the three compounds. The

lowest IC_{50} value (7μM) across all three compounds tested was obtained with ML334 for 3D7 indicating some aspect of the Dd2 genetic background, such as amplification of *Pfmdr1* or the chloroquine-resistance mutations in *Pfcrt,* may affect susceptibility to the ML334 compound.

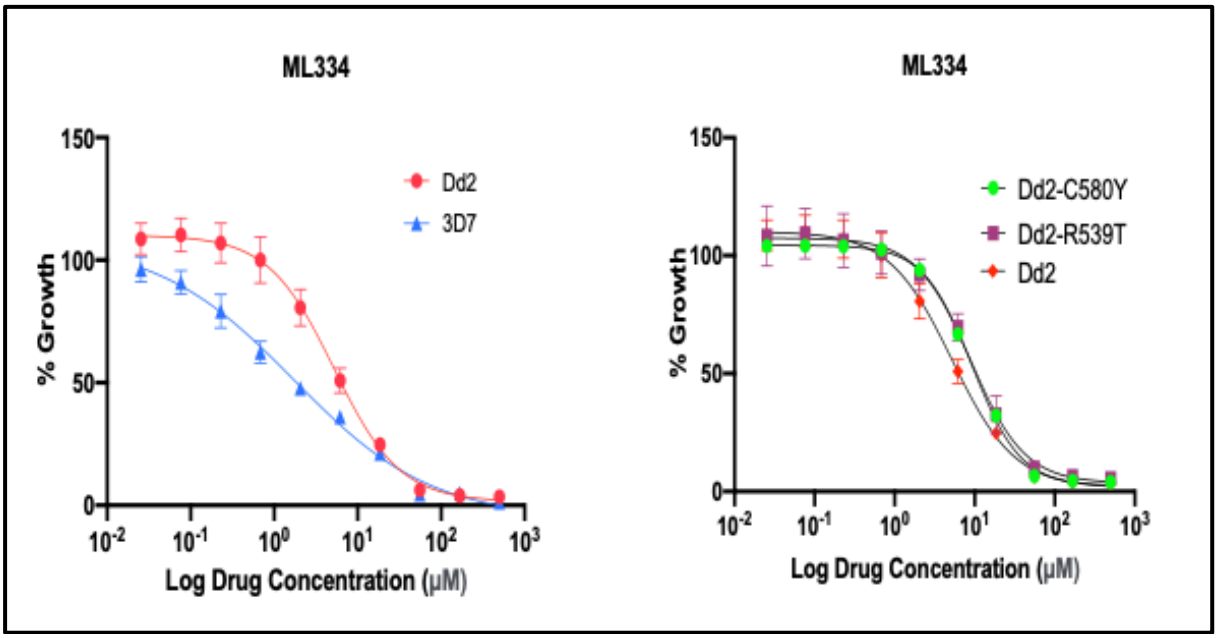

Figure 4.10 ML334 standard dose response curve. Dose response curves for the wild types (3D7 and Dd2) and Dd2 *Pfkelch13* mutants in assays performed in technical triplicates to obtain IC_{50} values

4. 4 Discussion

Resistance to antimalarial drugs that have emerged in *P. falciparum* parasites for different classes of antimalarials have been shown to occur upon exposure to strong selection with antimalarial treatments. Based on these previous trends, there is the expectation of the absence of resistance mechanisms for antimalarial candidates of classes different to the current ones (Ravenhall *et al,* 2019; Kidgell *et al,* 2006). Thus, the demonstrated sensitivity of the Dd2 mutant parasites Dd2-R539T and Dd2-C580Y to the kelch inhibiting compounds supports the importance of studying these compounds as drug candidates. This is highlighted by the activity against parasites growth in both wild type and mutant strains, demonstrated by all three KEAP1 kelch inhibiting compounds as observed in the results.

However, the drug resistance profiles that have been developed for the different antimalarials over the past years as well as geographical origin vary across different *P. falciparum* strains (Zhao *et al,* 2019; Anthony *et al,* 2016; Llinás *et al,* 2006). This can explain the varying results observed between 3D7 and Dd2 across the different compounds although both strains demonstrated moderate sensitivity to the compounds. These two strains have been shown to have varying drug resistance profiles. 3D7 is generally a sensitive strain but is however resistant to some antifolates (sulfadoxine), whereas Dd2 is a multi-drug resistant strain with *pfmdr1* copy number amplification and *pfcrt* point mutations (Corey *et al,* 2016).

This study describes the identification of human KEAP1 kelch inhibitors as having antimalarial activity, albeit with limited potency. However, the importance of these compounds to be studied as potential antimalarial drug candidates is based not on their overall potency but whether they could show a proof-of-principle differential activity against mutant *Pfkelch13*. The high level of structural similarity between

KEAP1 kelch and *Pfkelch13* highlights the importance of validating the activity of these compounds against *P. falciparum* parasites (Coppée *et al,* 2019; Li *et al,* 2004). C580Y and R539T are one of the major *Pfkelch13* mutations that have been implicated in artemisinin resistance (Chenet *et al,* 2017). Therefore, their sensitive phenotypes in the presence of two of the compounds tested indicates the potential to develop kelch inhibitors against resistant strains that may antagonise artemisinin resistance.

The occurrence of pre-existing resistance mechanisms and of rapid occurrence of resistance acquisition to new antimalarial compounds was shown in a previous cross-resistance study by Corey *et al,* (2016). These findings and existing antimalarial resistance patterns pose a big threat to both existing drugs and new drug candidates (Molnar *et al,* 2020; Corey *et al,* 2016). Screening of current antimalarial agents and compounds in development with parasites harbouring resistance-associated mutations facilitated by gene editing have provided important insights in drug resistance mechanisms and drug development (Ng and Fidock, 2019). Furthermore, there is a need for continued progress in identification of potential candidates for use in combination therapies due to the rapid resistance development pattern in malaria monotherapies. This has highlighted the importance of combination therapies in malaria chemotherapeutics which is the current recommendation for treatment, particularly ACTs (Gorka *et al,* 2013). Therefore, further work is needed in validating the potential of kelch inhibiting compounds as potential antimalarial candidates. The next steps towards this validation would be to perform experiments to assess if these potential kelch-interacting compounds are directly acting on the parasites through *Pfkelch13* or alternative modes of mechanism. This could be done using *Pfkelch13* knock down parasites (Birnbaum *et al,* 2020) that should sensitise the parasite to kelch13 inhibition, or more direct biochemical assays to look at binding such as surface

plasmon resonance. Techniques for assessing drug combination efficacies such as isobologram analyses, a widely used classic method for determining drug interactions (Huang *et al* 2019), could be performed to assess the interaction of these compounds and current frontline antimalarials such as artemisinin. Application of this method will help establish whether KEAP1 kelch inhibiting compounds tested in these experiments will exhibit antagonistic or synergistic drug efficacy properties when in combination with artemisinin. This will determine the potential suitability of *Pfkelch13* inhibitors as potential antimalarial candidates.

Although the general experiments for genome editing of the *P. falciparum* parasites were not completed due to Covid-related interruptions, parasites were recovered in transfections carried out on the Dd2 laboratory strain using the control plasmid by 16 days. The main limitation in the genome editing of field isolates is the length of time it takes for parasites to be recovered (Caro *et al,* 2012). This combined with the closure of the laboratories from the nationwide lockdown did not allow the continuity of the transfections. However, further work will be done to continue efficient transfection of different *P. falciparum* strains with the generated plasmid sub-pools of *Pfkelch13* 580 donors. This will facilitate the investigations on determining the factors driving the dominance of certain *Pfkelch13* mutations such as C580Y in certain backgrounds. The assessment of whether tolerance of the different mutations is driven by genetic backgrounds or co-existence of different mutations is needed. This assessment will be aided by successful transfection of field strains and genomic analysis. In the next steps, these experiments to provide important insight in understanding resistance patterns as well as enhancing transfection efficiency will be continued.